Supporting Information

Tetrahedral M^{II} based Binuclear Double-Stranded Helicates: Single-Ion-Magnet and Fluorescent Behaviour

Amit Kumar Mondal, Vijay Singh Parmar, Soumava Biswas, Sanjit Konar*

Department of Chemistry, IISER Bhopal, Bhopal By-Pass Road, Bhauri, Bhopal 462066, M. P., India.

Table S1. X-ray Crystallographic Data and Refinement Parameters for complexes **1**, **2**, **3** and **4**.

	1	**2**	**3**	**4**
Formula	$C_{56}H_{42}Co_2N_6O_6$	$C_{72}H_{70}Co_2N_{10}O_{10}$	$C_{57}H_{46}Zn_2N_6O_7$	$C_{68}H_{64}Zn_2N_8O_{10}$
M_w (g mol^{-1})	1012.82	1353.24	1057.78	1284.05
Crystal size (mm)	0.45×0.18×0.16	0.42×0.14×0.12	0.44×0.16×0.15	0.45×0.15×0.10
Crystal system	Triclinic	Monoclinic	Triclinic	Monoclinic
Space group	*P*-1	$P2_1/n$	*P*-1	*C*2/c
T (K)	140(2)	120(2)	140(2)	296(2)
a (Å)	10.563(5)	14.360(4)	14.061(4)	23.8383(8)
b (Å)	13.972(5)	20.040(5)	14.295(4)	13.1878(5)
c (Å)	18.013(6)	24.583(7)	14.799(4)	20.3490(6)
α (°)	67.788(10)	90	70.968(9)	90
β (°)	76.918(10)	103.796(8)	65.639(8)	110.454(2)
γ (°)	80.174(11)	90	70.068(9)	90
V (Å^3)	2386.6(16)	6871(3)	2487.0(12)	5993.9(4)
Z	2	4	2	4
ρ_{calcd} (g cm^{-3})	1.409	1.308	1.413	1.423
μ(MoKα) (mm^{-1})	0.754	0.548	1.025	0.869
F(000)	1044	2824	1092	2672
T_{max}, T_{min}	0.896, 0.840	0.936, 0.912	0.867, 0.831	0.927, 0.865
h, k, l range	$-12 \le h \le 12$, $-16 \le k \le 16$, $-21 \le l \le 21$	$-17 \le h \le 17$, $-24 \le k \le 24$, $-29 \le l \le 29$	$-19 \le h \le 19$, $-19 \le k \le 19$, $-20 \le l \le 20$	$-28 \le h \le 28$, $-15 \le k \le 15$, $-24 \le l \le 24$
Collected reflections	8495	12273	12655	5286
Independent reflections	6916	7614	9793	3946
Goodness-of-fit (GOF) on F^2	1.031	1.035	0.945	1.082
R1, wR2 ($I > 2\sigma I$)	0.0322, 0.0772	0.0641, 0.1332	0.0373, 0.1152	0.0621, 0.1747
R1, wR2 (all data)	0.0458, 0.0833	0.1231, 0.1632	0.0570, 0.1317	0.0824, 0.1901
CCDC Number	1429966	1429967	1429968	1429969

$R1 = \Sigma||Fo| - |Fc||/\Sigma|Fo|$ and $wR2 = |\Sigma w(|Fo|^2 - |Fc|^2)|/\Sigma|w(Fo)^2|^{1/2}$

Table S2. Bond distances (Å) around Co^{II} and Zn^{II} centers found in **1**, **2**, **3** and **4**.

1		**2**		**3**		**4**	
Co2 - O2	1.9031	Co2 – O5	1.9220	Zn1 – O4	1.9068	Zn1 – O2	1.9056
Co2 – O1	1.8975	Co2 – O6	1.9049	Zn1 – O3	1.9064	Zn1 – O8	1.9105
Co2 – N5	1.9882	Co2 – N4	2.0027	Zn1 – N2	2.0168	Zn1 – N1	2.0096
Co2 – N6	1.9914	Co2 – N3	1.9905	Zn1 – N1	2.0169	Zn1 – N3	2.0128
Co1 – O6	1.8947	Co1 – O2	1.9041	Zn2 – O2	1.9042	Zn1′ – O2′	1.9056
Co1 – O5	1.8974	Co1 – O1	1.9011	Zn2 – O1	1.9215	Zn1′ – O8′	1.9105
Co1 – N2	1.9964	Co1 – N1	1.9969	Zn2 – N5	2.0146	Zn1′ – N1′	2.0096
Co1 – N1	1.9833	Co1 – N2	1.9850	Zn2 – N6	2.0098	Zn1′ – N3′	2.0128

Table S3. Bond angles around Co^{II} and Zn^{II} centers found in **1**, **2**, **3** and **4**.

1		**2**		**3**		**4**	
O2 - Co2 - O1	116.00	O5 - Co2 – O6	110.04	O4 - Zn1 - O3	115.21	O2 - Zn1 - N1	95.86
O2 - Co2 - N5	124.01	O6 - Co2 – N3	130.16	O4 - Zn1 - N2	95.93	O2 - Zn1 - O8	108.75
O2 - Co2 - N6	96.13	O5 - Co2 – N3	95.19	O4 - Zn1 - N1	125.84	O2 - Zn1 - N3	128.65
O1 - Co2 - N5	96.19	O6 - Co2 – N4	95.48	O3 - Zn1 - N2	122.79	N1 - Zn1 - O8	133.14
O1 - Co2 - N6	123.96	O5 - Co2 – N4	128.51	O3 - Zn1 - N1	95.64	N1 - Zn1 - N3	97.96
N5 - Co2 - N6	102.09	N4 - Co2 – N3	101.30	N2 - Zn1 - N1	103.29	O8 - Zn1 - N3	96.68
O6 - Co1 - O5	117.80	O2 - Co1 – O1	118.50	O2 - Zn2 - O1	111.38	O2′ - Zn1′ - N1′	95.86
O6 - Co1 - N2	122.81	O2 - Co1 – N1	125.86	O2 - Zn2 - N5	96.38	O2′ - Zn1′ - O8′	108.75
O6 - Co1 - N1	95.44	O2 - Co1 – N2	95.68	O2 - Zn2 - N6	122.50	O2′ - Zn1′ - N3′	128.65
O5 - Co1 - N2	96.35	O1 - Co1 – N1	95.09	O1 - Zn2 - N5	129.49	N1′ - Zn1′ - O8′	133.14
O5 - Co1 - N1	120.74	O1 - Co1 – N2	121.46	O1 - Zn2 - N6	96.13	N1′ - Zn1′ - N3′	97.96
N2 - Co1 - N1	104.90	N1 - Co1 – N2	101.23	N5 - Zn2 - N6	103.42	O8′ - Zn1′ - N3′	96.68

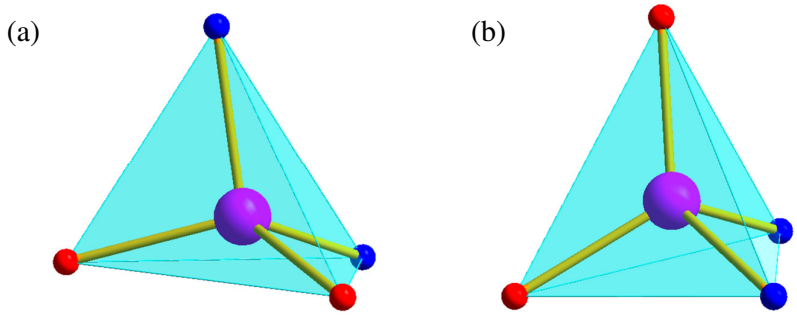

Fig. S1. Distorted tetrahedral coordination geometry around the Co^{II} centers in **1** (a) and **2** (b).

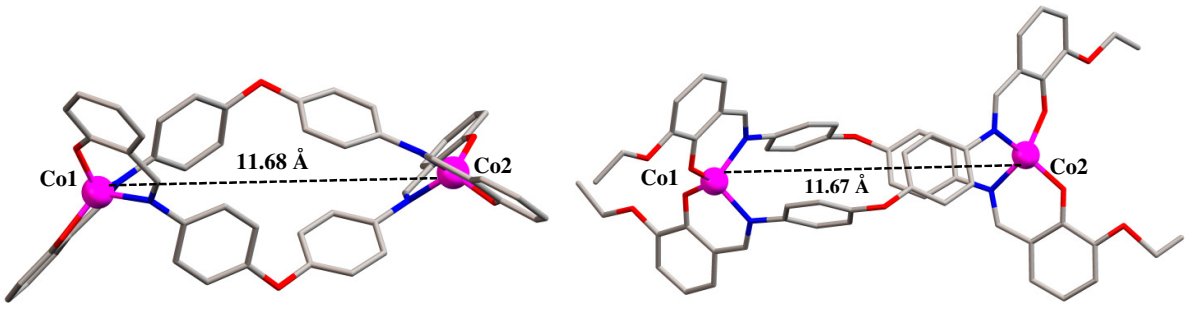

Fig. S2. Intramolecular Co···Co distances within the binuclear helicates found in complexes **1** (left) and **2** (right).

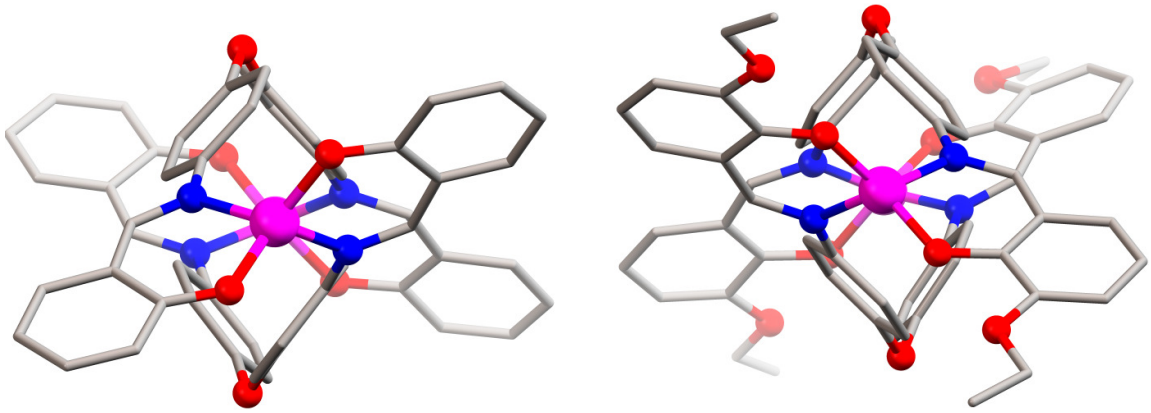

Fig. S3. A view down the Co···Co vector emphasizing the double stranded helical conformation of the complexes **1** (left) and **2** (right).

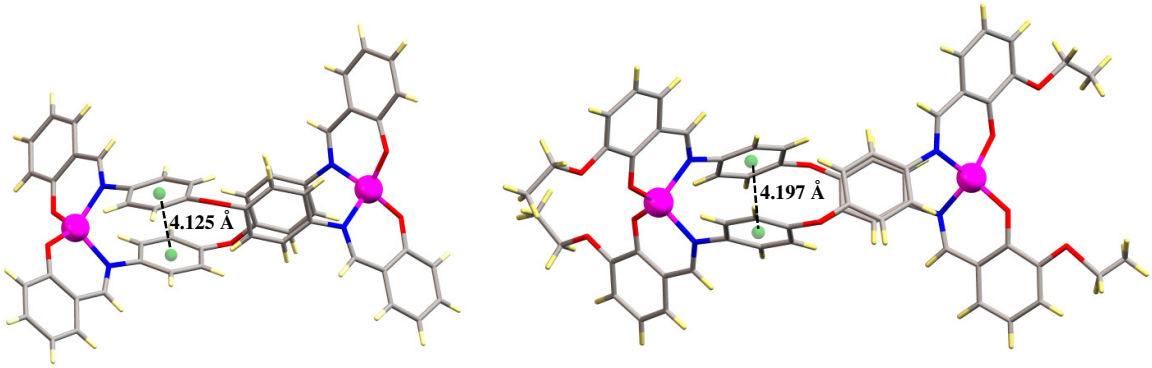

Fig. S4. Intramolecular π···π interactions between the phenyl rings within the double stranded helicates found in complexes **1** (left) and **2** (right).

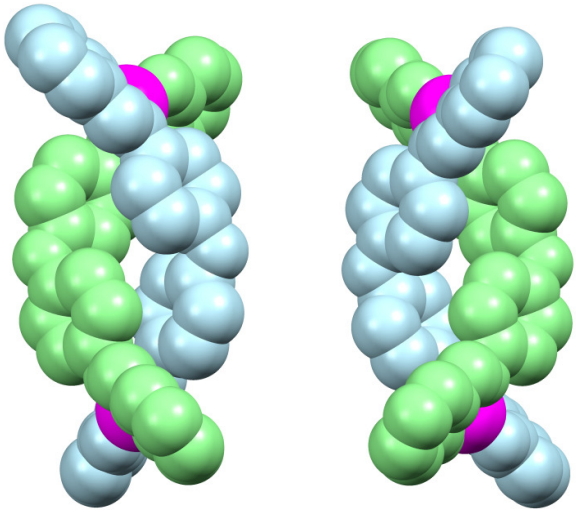

Fig. S5. Space-filling representations of the two independent $[Co_2(L^1)_2]$ complexes found in complex **1** with *M*- and *P*-helicity.

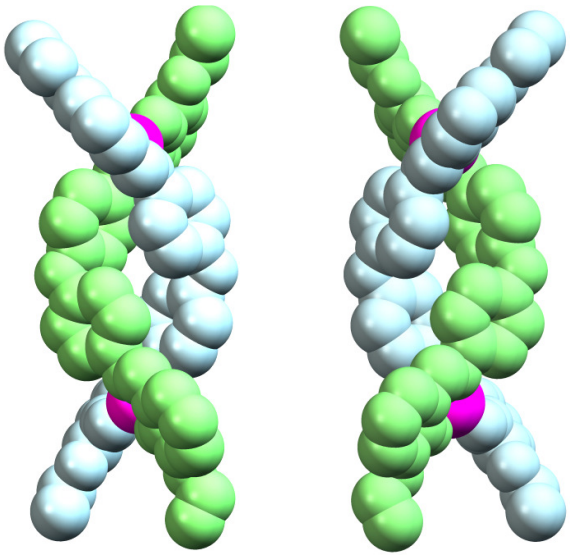

M *P*

Fig. S6. Space-filling representations of the two independent $[Co_2(L^2)_2]$ complexes found in complex **2** with *M*- and *P*-helicity.

Table S4. H-bond parameters found in complex **1.**

D–H···A	D–H(Å)	H···A(Å)	D···A (Å)	<D-H-A(°)	Symmetry[#]
C39-H39···O2	0.950	2.915	3.704	141.26	0
C32-H32···O6	0.950	2.877	3.675	142.25	0
C20-H20···O5	0.950	2.939	3.673	135.09	0
C36-H36···N4	0.950	2.631	3.498	151.98	0
C25-H25···N4	0.950	2.671	3.436	137.86	0
C50-H50···O1	0.950	2.971	3.459	113.30	1
C56-H56···O1	0.950	2.694	3.263	119.08	1
C27-H27A···O2	0.950	2.728	3.501	136.11	1
C43-H43···O2	0.950	2.828	3.263	108.93	2
C14-H14···N4	0.950	2.541	3.467	164.98	3
C2-H2···N3	0.950	2.883	3.639	137.39	4
C55-H55···O5	0.950	2.803	3.473	128.33	5
C54-H54···O6	0.950	2.649	3.538	155.99	5
C47-H47···O6	0.950	2.791	3.480	130.19	6
C47-H47···O5	0.950	2.801	3.576	139.37	6

(0) x,y,z (1) -x+1,-y+1,-z+2 (2) -x,-y+1,-z+2 (3) -x+1,-y+2,-z+1 (4) -x+1,-y+1,-z+1 (5) x,+y,+z+1 (6) x,+y-1,+z+1

Table S5. H-bond parameters found in complex **2**.

D– H···A	D–H(Å)	H···A(Å)	D···A (Å)	<D-H-A(°)	Symmetry[#]
C7-H7···O1	0.951	2.778	3.580	142.53	0
C68-H68···N1S	0.951	2.765	3.666	158.44	0
C79-H79A···N1S	0.990	2.889	3.547	124.64	0
C9-H9···N2S	0.950	2.575	3.523	175.72	1
C43-H43···N2S	0.950	2.843	3.709	152.07	1
C50-H50···O10	0.949	2.818	3.475	127.17	2
C51-H51···O10	0.951	2.919	3.530	123.17	2
C65-H65···O8	0.950	2.747	3.632	155.16	3
C52-H52···O6	0.949	2.718	3.108	105.36	3
C52-H52···O8	0.949	2.669	3.565	157.59	3
C57-H57···N4	0.950	2.824	3.567	135.79	4
C61-H61···O4	0.949	2.970	3.823	150.24	5
C72-H72···O10	0.951	2.987	3.884	157.86	6

(0) x,y,z; (1) -x+1,-y+1,-z; (2) x-1/2,-y+1/2,+z-1/2; (3) –x+2,-y+1,-z; (4) –x+3/2,+y-1/2,-z+1/2; (5) –x+1,-y,-z; (6) x+1,+y,+z.

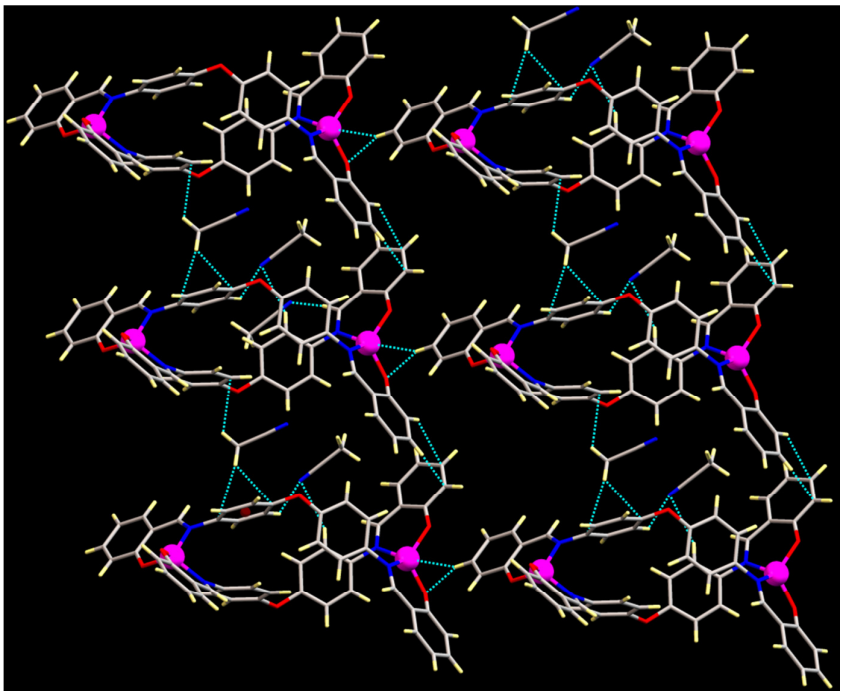

Fig. S7. A view of supramolecular 2D arrangement of complex **1** through intermolecular H-bonding and CH···π interactions.

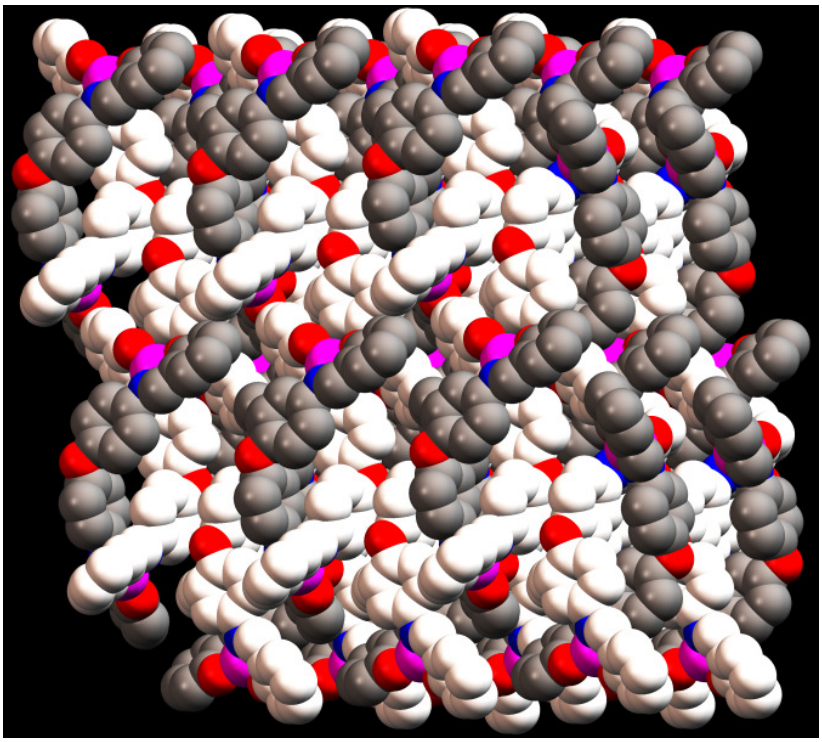

Fig. S8. A view of de-solvated framework of **1** emphasizing the supramolecular interactions.

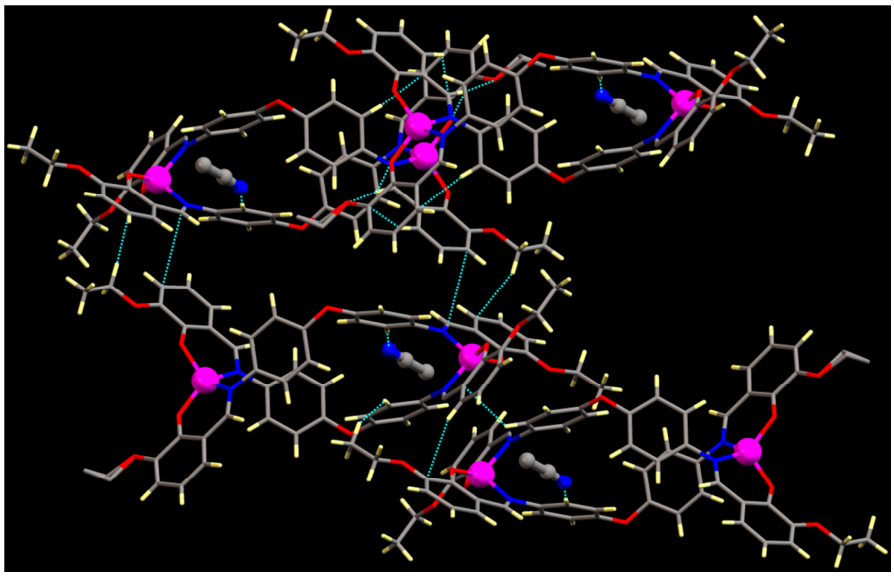

Fig. S9. A view of supramolecular 2D arrangement of complex **2** through intermolecular H-bonding and CH···π interactions.

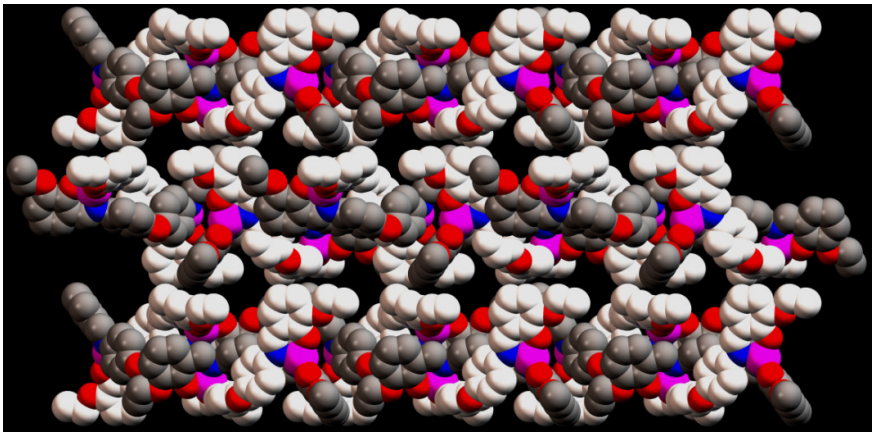

Fig. S10. A view of de-solvated framework of **2** emphasizing the supramolecular interactions.

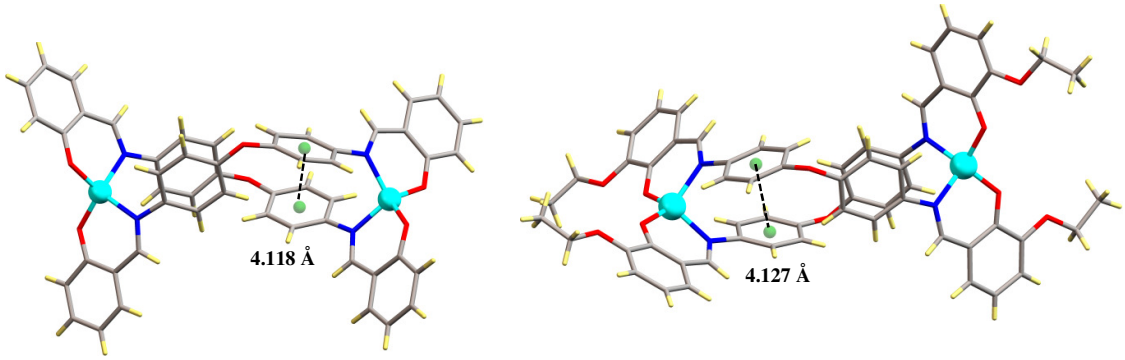

Fig. S11. Intramolecular π···π interactions between the phenyl rings within the double stranded helicates found in complexes **3** (left) and **4** (right).

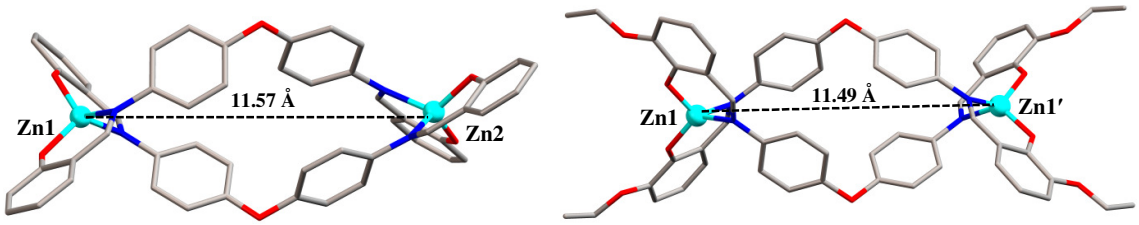

Fig. S12. Intramolecular Zn···Zn distances within the binuclear helicates found in complexes **3** (left) and **4** (right).

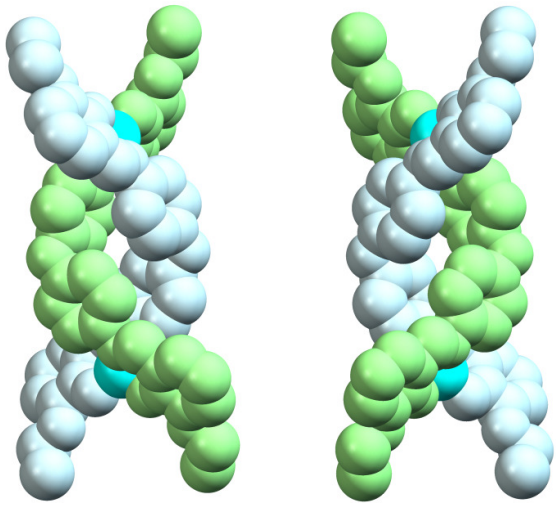

M *P*

Fig. S13. Space-filling representations of the two independent $[Zn_2(L^2)_2]$ complexes found in complex **4** with *M*- and *P*-helicity.

Table S6. H-bond parameters found in complex **3**.

D–H···A	D–H(Å)	H···A(Å)	D···A (Å)	<D-H-A(°)	Symmetry#
O8-H8A···O1	0.84	2.05	2.881	173	0
C1-H1···N7	0.950	2.46	3.379	164	0
C4-H4···N8	0.950	2.62	3.571	175	2
C49-H49···O3	0.950	2.58	3.327	136	1
C53-H53A···O8	0.98	2.59	3.535	162	3
C55-H55B···O8	0.98	2.51	3.247	132	3
C80-H80C···O2	0.98	2.57	3.423	146	0

(0) x,y,z (1) x,-1+y,1+z (2) 1-x,1-y,-z (3) 1-x,1-y,1-z

Table S7. H-bond parameters found in complex **4.**

D–H···A	D–H(Å)	H···A(Å)	D···A (Å)	<D-H-A(°)	Symmetry#
C45-H45···O2	0.930	2.996	3.784	143.47	1
C50-H50···O8	0.930	2.989	3.795	145.79	1
C38-H38···O6	0.930	2.508	3.323	146.43	2
C37-H37···O2	0.930	2.892	3.304	108.27	3
C53-H53B···O9	0.960	2.708	3.655	168.96	4

#.(1) -x+1,+y,-z+1/2 (2) x-1/2,+y-1/2,+z (3) x-1/2,-y+1/2,+z-1/2 (4) -x+1,-y+1,-z+1

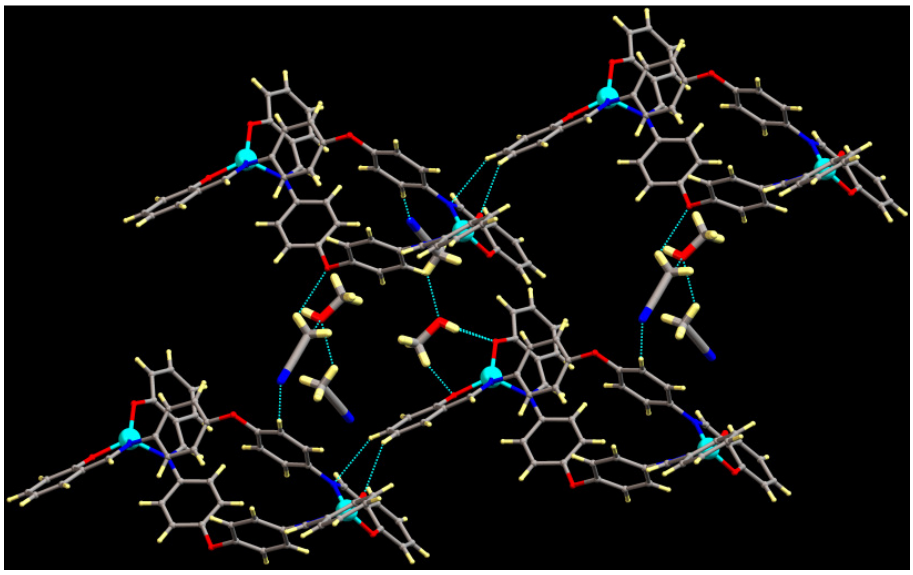

Fig. S14. A view of supramolecular 2D arrangement of complex **3** through intermolecular H-bonding interactions.

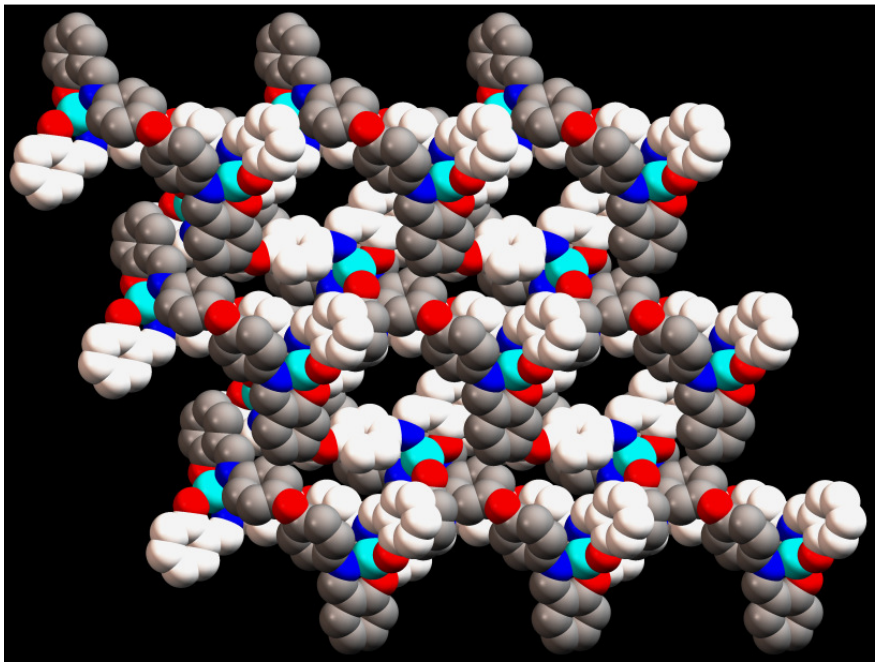

Fig. S15. A view of de-solvated framework of **3** emphasizing the supramolecular interactions.

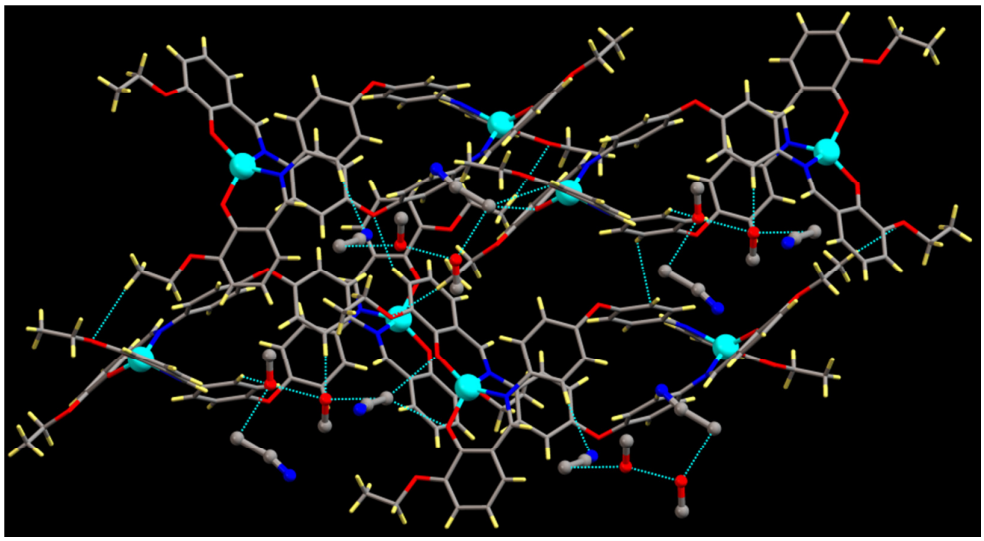

Fig. S16. A view of supramolecular 2D arrangement of complex **4** through intermolecular H-bonding interactions.

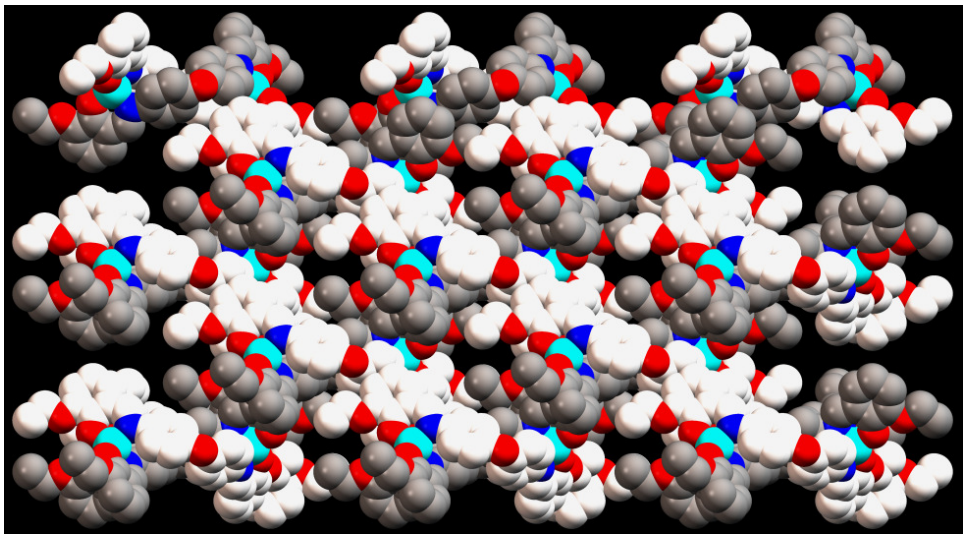

Fig. S17. A view of de-solvated framework of **4** emphasizing the supramolecular interactions.

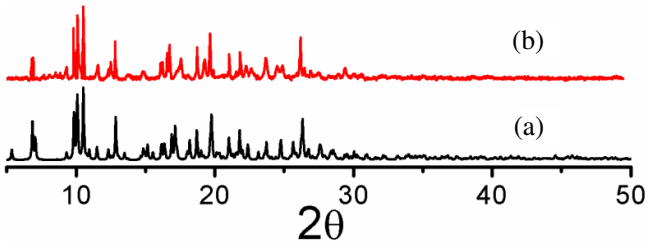

Fig. S18. PXRD patterns of **1**; (a) simulated, (b) as-synthesized.

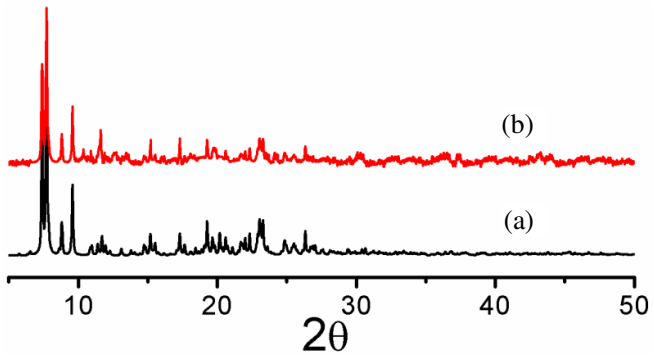

Fig. S19. PXRD patterns of **2**; (a) simulated, (b) as-synthesized.

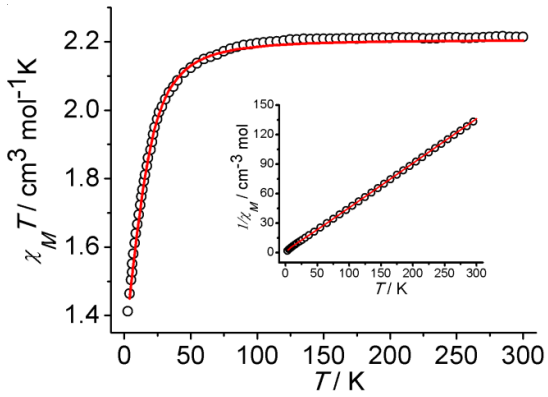

Fig. S20. $\chi_M T$ *vs.* T plot measured at 0.1 T for complex **1** and $1/\chi_M$ *vs.* T plot shown in the inset. The red lines are the best fit.

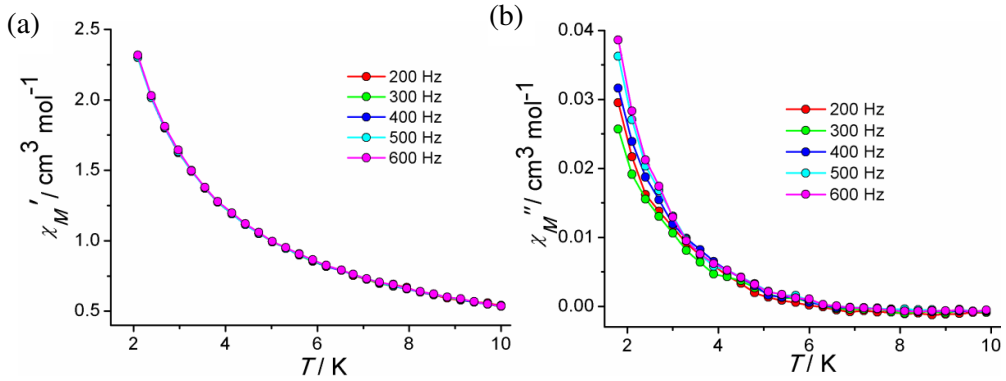

Fig. S21. (a) In-phase (χ_M') and (b) Out-of-phase (χ_M'') AC magnetic susceptibility plots for complex **1** at 0 Oe.

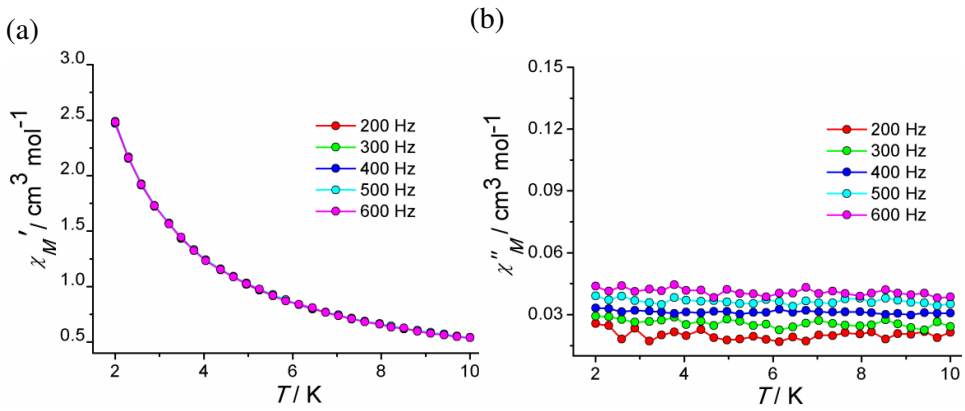

Fig. S22. (a) In-phase (χ_M') and (b) Out-of-phase (χ_M'') AC magnetic susceptibility plots for complex **2** at 0 Oe.

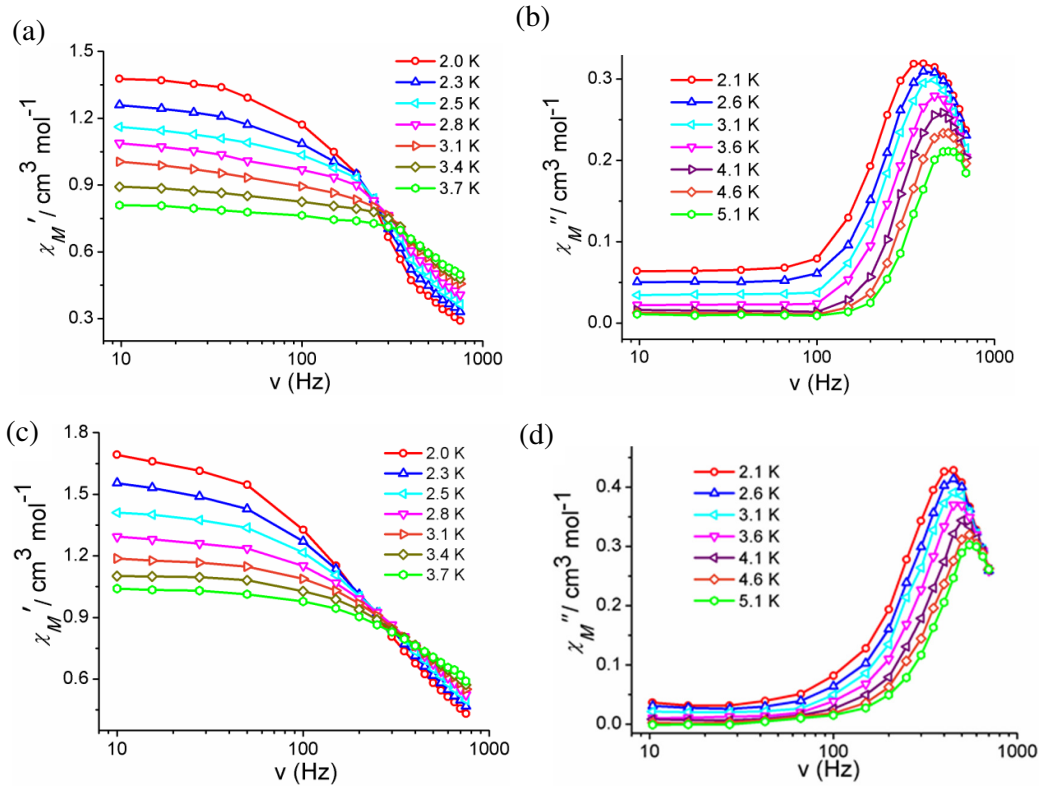

Fig. S23. Frequency dependency of the in-phase (a and c) and out-of phase (b and d) ac susceptibility plots for complexes **1** and **2** under 1000 Oe dc field.

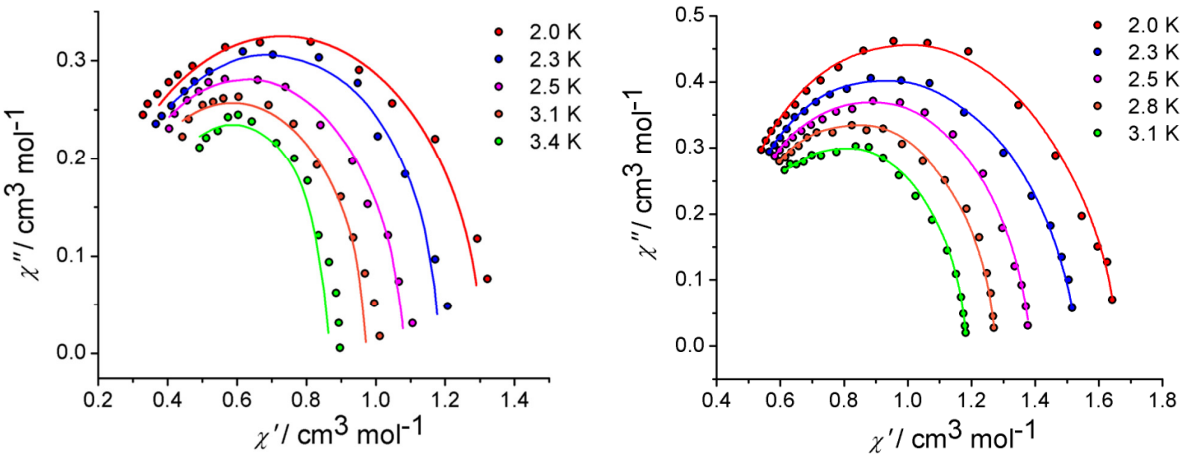

Fig. S24. Cole-Cole plots for complex **1** (left) and **2** (right). Solid lines represent the best fit.

(a)

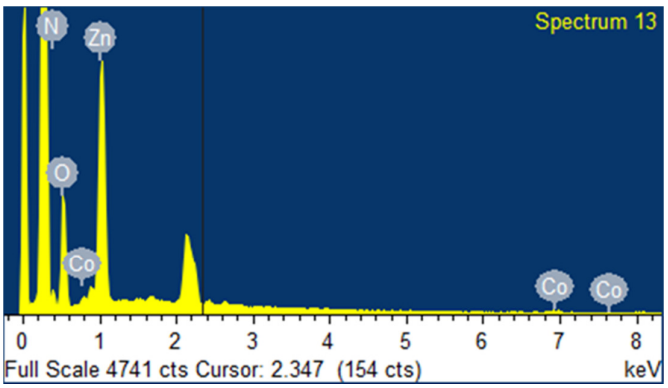

(b)

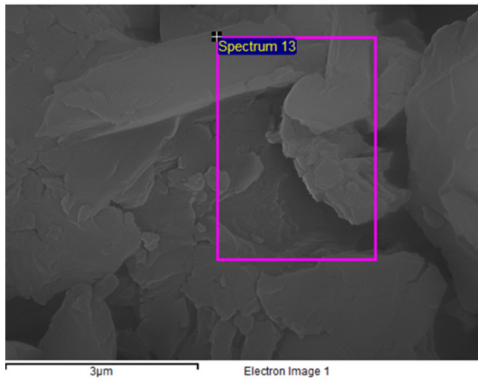

(c)

Element	N	O	Co	Zn	Total
Weight%	14.06	42.17	2.65	41.12	100.00

Fig. S25. (a) EDS, and (b) SEM image of diluted sample, (c) elemental analysis from EDS.

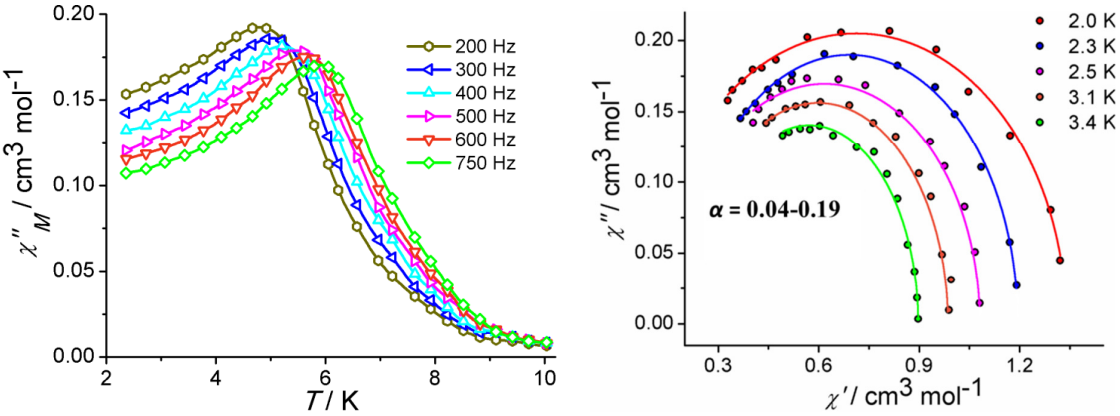

Fig. S26. Out-of-phase (χ_M'') ac magnetic susceptibility plot for diluted sample at 1000 Oe dc field (left) and Cole-Cole plots for diluted sample (right). Solid lines represent the best fit.

Shape analysis

Table S8: Summary of SHAPE analysis around Co^{II} centers of complex **1** and **2**.

SP-4	1	D_{4h}	Square
T-4	2	T_d	Tetrahedron
SS-4	3	C_{2v}	Seesaw
vTBPY-4	4	C_{3v}	Vacant trigonal bipyramid

Complex **1**:

Structure	[ML_4]	SP-4	T-4	SS-4	vTBPY-4
Co1	,	22.139,	**2.150**,	6.399,	4.989,

Complex **2**:

Structure	[ML_4]	SP-4	T-4	SS-4	vTBPY-4
Co1	,	18.301,	**3.345**,	5.568,	6.379,

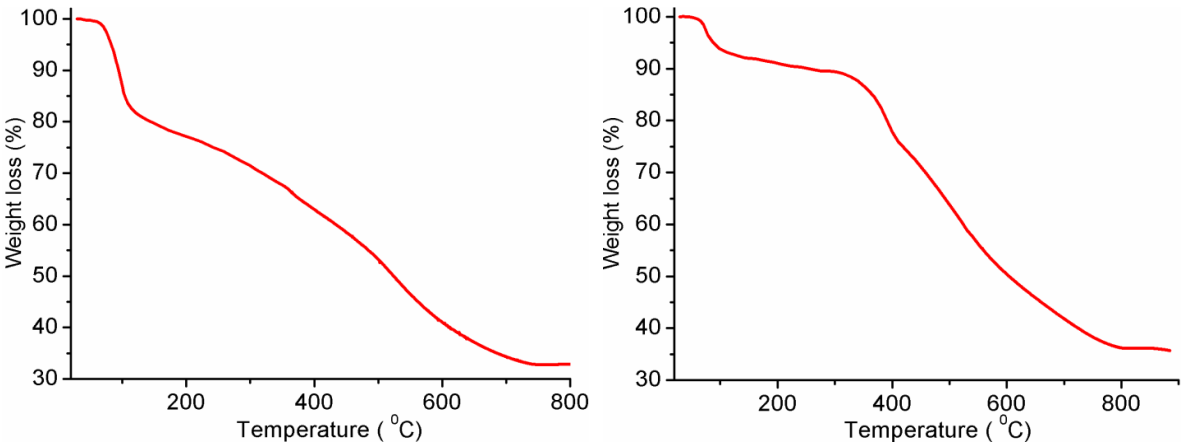

Fig. S27. Thermogravimetric profiles for complexes **2** (left) and **4** (right).